Thymic precursors to the Mucosal-Associated Invariant T cell lineage

Hui Fern Koay[1], Nicholas A Gherardin[1,2], Anselm Enders[3], Liyen Loh[1], Zhenjun Chen[1], Alexandra J. Corbett[1], Sidonia B.G. Eckle[1], Bronwyn Meehan[1], Yves d'Udekem[4], Igor Konstantinov[4], Martha Lappas[5], Ligong Liu[6], Chris C. Goodnow[3], David P Fairlie[6,7], Jamie Rossjohn[8,9,10], Katherine Kedzierska[1], Stuart P. Berzins[11], James McCluskey[1], Adam P. Uldrich[1,12], Dale I. Godfrey*[1,12], Daniel G. Pellicci*[1,12]

*joint senior authors.

Correspondence: Dale Godfrey, godfrey@unimelb.edu.au, Daniel Pellicci, pellicci@unimelb.edu.au.

[1]Department of Microbiology and Immunology, Peter Doherty Institute for Infection and Immunity, University of Melbourne, Parkville, Victoria 3010, Australia.

[2]Cancer Immunology Research Program, Peter MacCallum Cancer Centre, East Melbourne, Victoria 3002, Australia

[3]John Curtin School of Medical Research, Department of Immunology, Canberra, ACT, Australia.

[4]Royal Children's Hospital, Flemington Road, Parkville, Melbourne, Victoria, 3052, Australia.

[5]Obstetrics, Nutrition and Endocrinology Group, Department of Obstetrics and Gynaecology, University of Melbourne, Heidelberg, Victoria, Australia; Mercy Perinatal Research Centre, Mercy Hospital for Women, Heidelberg, Victoria, Australia.

[6]Institute for Molecular Bioscience, University of Queensland, Brisbane, Qld 4072, Australia.

[7]Australian Research Council Centre of Excellence for Advanced Molecular Imaging, University of Queensland, Brisbane, Qld 4072, Australia.

[8]Department of Biochemistry and Molecular Biology, School of Biomedical Sciences, Monash University, Clayton, Victoria 3800, Australia

[9]Institute of Infection and Immunity, Cardiff University, School of Medicine, Heath Park, Cardiff CF14 4XN, UK

[10]Australian Research Council Centre of Excellence for Advanced Molecular Imaging, Monash University, Clayton, Victoria 3800, Australia.

[11]Federation University, Ballarat, Victoria, Australia; Fiona Elsey Cancer Research Institute, Ballarat, Victoria, Australia

[12]Australian Research Council Centre of Excellence for Advanced Molecular Imaging, University of Melbourne, Parkville, Victoria 3010, Australia.

Running title: MAIT cell development.

T cells play key roles in the immune system by detecting microbial molecules associated with infection. One major T cell population, mucosal-associated invariant T (MAIT) cells, are activated by microbial vitamin B2 (riboflavin) derivatives presented by the major histocompatibility complex (MHC) class I related protein, MR1[1-4]. In humans, MAIT cells represent between 5 and 50% of T cells in different human tissues [5-8]. The number of MAIT cells varies widely between individuals and the factors that govern the development of these cells are unclear. Using MR1 tetramers to detect MAIT cells in mice and humans, we have now identified thymic precursors to the MAIT cell lineage and delineated three distinct stages in MAIT cell development. In mice, the least mature, stage 1 (CD24$^+$CD44$^-$) cells progress to an intermediate stage 2 (CD24$^-$CD44$^-$) before maturing into stage 3 (CD24$^-$CD44$^+$) MAIT cells. Progression through each of these checkpoints is MR1 dependent, while the final maturation checkpoint that gives rise to functional MAIT cells requires the transcription factor, promyelocytic leukemia zinc finger (PLZF). In humans, stage 1 (CD161$^-$CD27$^-$) and stage 2 MAIT cells (CD161$^-$CD27$^+$) predominate in the thymus, while stage 3 cells (CD161$^+$) progressively increase in percentage in umbilical cord blood, young peripheral blood and adult peripheral blood. MAIT cell maturation can also occur after thymic emigration of immature MAIT cells in both humans and mice. Accordingly, this study maps the intrathymic developmental pathway and identifies key checkpoints that control the maturation of functional MAIT cells in mice and humans.

Recent studies have indicated that MAIT cells play unique and important roles in the immune system in response to infection with a broad range of pathogens[6,9,10] and they may also be involved in autoimmunity and other inflammatory responses[24]. Previous studies have demonstrated that MAIT cells are thymus dependent[4], MR1-restricted cells[1], that undergo positive selection and lineage commitment upon interaction with MR1-expressing CD4$^+$CD8$^+$ cortical thymocytes[11]. With the recent development of MR1 tetramers loaded with riboflavin derivatives such as 5-OP-RU [2,12,13,15], it is now possible to specifically identify and isolate MAIT cells in mice and humans. Here, we examined the developmental pathway of MAIT cells, and identified a previously undescribed population of CD24$^+$CD44$^-$ MAIT cells in mouse thymus but not in peripheral organs, where essentially all MAIT cells were CD24$^-$CD44$^+$ (Figure 1a). Single cell TCR sequence analysis of both populations of thymic MAIT cells showed that they utilized an invariant Vα19Jα33 (TRAV1 TRAJ33) TCR-α chain, paired with a limited range of TCR-β chains (TRBV13 and TRBV19) that are characteristic of the MAIT cell lineage[4] (Supplementary Table 1). Characterisation of

CD24$^+$CD44$^-$ and CD24$^-$CD44$^+$ MAIT cells within the thymus revealed contrasting phenotypes (Figure 1b and Supplementary Table 2). CD24$^+$CD44$^-$ MAIT cells expressed low levels of PLZF, CD103, CD122 (IL-2Rβ), CD127 (IL-7Rα), CD218 (IL-18R), CD278 (ICOS) and CD161 (NK1.1), but higher levels of CD62L and CD69 compared to CD24$^-$CD44$^+$ MAIT cells (Figure 1b). Enrichment of thymic MR1-5-OP-RU tetramer$^+$ cells identified an additional small subpopulation of CD24$^-$CD44$^-$ MAIT cells (Figure 1c), thus, we tentatively defined these populations as stage 1 (CD24$^+$CD44$^-$), stage 2 (CD24$^-$CD44$^-$) and stage 3 (CD24$^-$CD44$^+$) MAIT cells (Figure 1). Analysis of forward scatter (FSC), CD4 and CD8 expression on these thymic MAIT cell populations showed that the vast majority of stage 1 MAIT cells were small and CD4$^+$ or CD4$^+$CD8$^+$, a phenotype that is typically associated with immature cells in the thymus and that also defines the earliest stage in the development of CD1d-restricted Natural Killer T (NKT) cells[14]. Stage 2 cells were slightly larger, mostly CD4$^+$CD8$^-$, whereas stage 3 MAIT cells were the largest and resemble mature MAIT cells in peripheral organs, being mostly CD4$^-$CD8$^-$ or CD8$^+$ (Figure 1c). Collectively, our data supports the presence of at least three distinct stages of MAIT cell development within mouse thymus.

To investigate their developmental progression, we carried out an ontogeny study for MAIT cell subsets in mouse thymus at 2, 4 and 8 weeks of age. Stage 1 MAIT cells were the major subset (>50%) in the very young mouse thymus at 2 weeks, declining to ~30% at 4 weeks and just ~10% of total thymic MAIT cells in the adult 8 week old mouse thymus (Figure 2a and b). Conversely, the proportion of stage 3 MAIT cells was low (~20%) at 2 weeks and gradually increased with age (~60% at 4 weeks and ~80% at 8 weeks) (Figure 2a and b), supporting the developmental progression of MAIT cells from stage 1 to stage 3. To determine at which stage MAIT cells gain functional maturity, we examined the three maturation stages for production of IL-17 and IFN-γ, cytokines typically expressed by mouse MAIT cells following stimulation[15]. Only the most mature, stage 3 MAIT cells from the thymus produced cytokines in this assay (Figure 2c). Accordingly, the loss of CD24 and the acquisition of CD44 correlate with the functional potential of mouse MAIT cells.

To directly investigate the precursor/progeny relationship of these subsets, we established an *in vitro* MAIT cell development system, using an adaptation of the OP9 cell-thymocyte co-culture system[16]. Because the numbers of thymus MAIT cell subsets in wild type mice were very low, we initially used Vα19 TCR transgenic Cα$^{-/-}$ mice where the three stages of thymus MAIT cells were far more abundant (Supplementary Figure 1), thus allowing us to isolate sufficient numbers of these cells for

in vitro differentiation studies. After 5 days of co-culture with OP9 cells, purified stage 1 MAIT cells had started to differentiate into stage 2 and stage 3 cells (Figure 2d and e). Similarly, the stage 2 cells had progressed further toward stage 3, whereas the stage 3 cells maintained their mature CD24$^-$ CD44$^+$ phenotype (Figure 2d and e). Importantly, in control cultures lacking OP9 cells, no MAIT cell differentiation was observed, indicating the importance of stromal cell-derived factors in the MAIT cell differentiation process. We also tested OP9 cells engineered to express the Notch ligand, Delta-like 1, (OP9-DL1). Similar to the maturation of γδ T cells from γδTCR-expressing T cell precursors[17], signalling through DL1 was not required for maturation of TCR$^+$ MAIT cell precursors (data not shown) hence, parental OP9 cells were used for subsequent experiments. The presence of anti-MR1 blocking antibody completely inhibited the progression of stage 1 to stage 3 MAIT cells, and partially inhibited the differentiation or survival of stage 2 and stage 3 cells, as reflected by a sharp reduction in cell numbers by the end of culture (Figure 2d and e). These data are consistent with the lack of MAIT cells in MR1-deficient mice [1,8,15], but also highlight that the expression of MR1 is critical for both the initial development and further differentiation of MAIT cells.

Having established this differentiation sequence using Vα19 TCR transgenic MAIT cells, we next undertook similar experiments using MAIT cell subsets from wild type mice (Figure 2d). Because these cells were much less frequent, we were unable to isolate sufficient numbers of the intermediate stage 2 cells, but nonetheless, the results of culturing stage 1 and stage 3 MAIT cells matched those observed with the Vα19 TCR transgenic cells (Figure 2d and e). Thus, stage 1 cells progressed to stages 2 and 3 after 5 days of co-culture with OP9 cells, whereas stage 3 cells maintained their mature phenotype. Taken together, these data confirm that differentiation of mouse MAIT cells can be defined by a three-stage sequential pathway from CD24$^+$CD44$^-$ (stage 1), via CD24$^-$CD44$^-$ (stage 2), to CD24$^-$CD44$^+$ (stage 3).

The transcription factor PLZF, known to be important for the development of NKT cells, ILC cells and some γδ T cells[18-21] is expressed by MAIT cells in humans and mice[8,15]. We recently determined that the production of normal numbers of MAIT cells depends upon this factor, although notably, a residual population of MAIT cells remained in PLZF-deficient mice[15]. Using wild type mice, we determined that this transcription factor is first expressed on stage 2 MAIT cells, which were heterogeneous for PLZF expression, and fully expressed by stage 3 (Figure 3a). Examination of PLZF knockout (KO) mice revealed that the stage 1 and stage 2 MAIT cell compartments were intact, whereas stage 3 MAIT cells were completely absent (Figure 3b and c). Even in peripheral

tissues, the residual MAIT cells were also blocked at stage 2 including a predominantly CD4$^+$CD8$^-$ phenotype (Figure 3b), and lack of CD218, CD127 and CD103 expression (data not shown), thus resembling immature MAIT cells as shown in (Figure 1b). This suggests that the progression to stage 2 is PLZF independent but maturation of stage 2 to stage 3 is absolutely dependent on PLZF, and furthermore this can occur after stage 2 cells leave the thymus. In the absence of the PLZF driven maturation signal, stage 2 MAIT cells remain immature in both thymus and peripheral tissues.

Given that MAIT cells in mouse thymus could be delineated into three phenotypically and functionally distinct stages, it was important to determine whether MAIT cells followed a similar developmental pathway in humans. Our initial studies involved using human MR1-5-OP-RU tetramers along with surrogate phenotypic markers Vα7.2, CD161 and CD218, which are commonly used to identify MAIT cells in humans[5,8,13,22-24]. We detected MAIT cells (defined as Vα7.2$^+$ MR1-5-OP-RU tetramer$^+$) in all human thymus samples tested, and found these cells to be much less frequent (<0.05%) than in adult human blood where they typically represent 2-5% of T cells (Figure 4a and [15]), and they were therefore difficult to detect amongst whole thymocyte preparations. However, when we enriched for Vα7.2$^+$ cells using magnetic bead enrichment, a clear population of MAIT cells was detected, ranging from 0.08-0.45% of Vα7.2$^+$ thymocytes (Figure 4a and b). Examination of thymic MAIT cells for CD161 and CD218 revealed a markedly distinct cell surface phenotype compared to those from adult peripheral blood, umbilical cord blood and matched young peripheral blood taken from the thymus donors. The vast majority of MAIT cells from the blood of adult and young donors co-expressed CD218 and CD161 at high levels and were predominantly CD4$^-$CD8$^-$ or CD4$^-$CD8$^+$ (Figure 4a), consistent with previous findings[5,8,13,23]. In contrast, the vast majority of MAIT cells from the thymus were CD218$^-$CD161$^-$, ranging from 40-97% of all thymic MAIT cells (Figure 4a and b), suggesting that CD218$^-$CD161$^-$ MAIT cells represent a major immature precursor population within human thymus.

These results showed a clear and significant difference in the phenotype of MAIT cells, based on expression of CD218 and CD161 and CD4/CD8 co-receptor expression in human thymus compared to donor-matched peripheral blood (Figure 4a-d). These observations strongly suggest that MAIT cells in the thymus are predominantly immature and that further maturation, either just prior to, or soon after, thymic emigration occurs in humans. To further investigate where this maturation occurs, we examined cord blood samples as a source of MAIT cells, since in this compartment they should be enriched for recent thymic emigrants (Figure 4a-c). MAIT cells were detectable in all samples,

albeit at low frequencies ranging from 0.006-0.02% of total cells (0.3-0.9% of $V\alpha7.2^+$ T cells), and were therefore similar to thymus and distinct from adult peripheral blood in terms of frequency (Figure 4a and b). These cells were heterogeneous for CD218 and CD161 and expressed higher proportions of $CD4^+$, but lacked $CD4^+CD8^+$ MAIT cells (Figure 4a). Thus, MAIT cells that have recently emigrated from the thymus were a mixture of immature thymus-like cells and mature, peripheral blood-like cells.

Immature $CD161^-$ MAIT cells could be further divided based on CD27 expression, allowing us to fractionate MAIT cells into three stages that closely resembled their mouse counterparts. $CD161^-CD27^-$ MAIT cells were mostly $CD4^+$ or $CD4^+CD8^+$, $PLZF^{lo}$, and were only detected in human thymus (Figure 4a, e and f). $CD161^-CD27^+$ MAIT cells appeared to be more mature with less $CD4^+CD8^+$ and more $CD4^-CD8^+$; they expressed low to intermediate levels of PLZF, and they were detected at low frequency in cord blood (22±2%) and young blood (13±4%) but were essentially absent from adult blood (0.9±0.3%) (Figure 4a, d and f). In contrast, $CD161^+CD27^{+/-}$ MAIT cells were mostly $CD4^-CD8^-$ or $CD8^+$ (Figure 4f), $PLZF^+$, and were very similar to MAIT cells found in human peripheral blood (Figure 4a). Taken together, these data suggested that $CD161^-CD27^-$ MAIT cells are the least mature (stage 1), followed by $CD161^-CD27^-$ cells (stage 2) that are capable of emigrating from the human thymus and continuing their maturation extrathymically, giving rise to $CD161^+CD27^{+/-}$ (stage 3) cells, that resemble MAIT cells detected in adult peripheral tissues. This is reminiscent of CD1d-restricted NKT cells in humans, which also undergo their final maturation (upregulation of CD161 and downregulation of CD4) extrathymically[25]. Based on the large increase in the frequency of MAIT cells after they leave the thymus, it is likely that their numbers increase in the periphery, possibly in response to microbial antigens, as has been previously reported in mice[1]. Our data provide a very different perspective of human MAIT cell development to that of two previous studies where immature MAIT cells were described as predominantly $CD4^-$ [8,26]. This is likely due to the use of surrogate phenotypic markers such as $CD161^+$ and $V\alpha7.2^+$, which would exclude the vast majority of immature MAIT cells or include non-MAIT cells.

We have defined thymic precursors for the MAIT cell lineage and mapped a three-stage developmental pathway for MAIT cell development and maturation in mice and humans. We propose that these transitions are regulated by developmental checkpoints (Supplementary Figure 2): Checkpoint 1 occurs in the thymus, and controls initial commitment to the MAIT cell lineage (stage 1 MAIT cells) and is absolutely dependent on MR1; Checkpoint 2 (transition from stage 1 to stage 2)

also occurs in the thymus and requires ongoing interactions with MR1 as well as stromal cell factors; Checkpoint 3, governs the final maturation step from stage 2 to stage 3, is absolutely dependent on the transcription factor PLZF and requires ongoing contact with MR1 for optimal efficiency, but this transition can occur both intrathymically and extrathymically (Supplementary Figure 2). In summary, our study has mapped a three-stage, three-checkpoint process for MAIT cell development, and will serve as the basis for understanding the impact of factors that regulate this highly abundant, yet highly variable, T cell lineage.

Methods

Mice.

C57BL/6 (B6) mice, MR1 KO mice, and Vα19 TCR transgenic Cα-/- mice (all on a C57BL/6 background) were bred in house at the Department of Microbiology and Immunology Animal House, University of Melbourne. PLZF KO mice were generated and bred in house at the John Curtin School of Medical Research as previously described (15). All procedures using mice were approved by the University of Melbourne Animal Ethics Committee or the Australian National University Animal Experimentation Ethics Committee. Single cell suspensions from mouse thymus, spleen, lung and inguinal lymph nodes were prepared as previously described[15].

Human blood and tissue

Adult peripheral human blood samples were obtained from the Australian Red Cross Blood Service under agreement number 13-04VIC-07. Young human peripheral blood samples and matching thymus (young donors ranged from 2 days to 12 years of age) were obtained from the Royal Children's Hospital (RCH), Victoria, Australia. Umbilical cord blood samples were obtained from the Mercy Hospital for Women, Victoria, Australia. Experiments were conducted in accordance with University of Melbourne Human Research and Ethics committee guidelines (reference numbers 1035100 and 1443540), Mercy Health Human Research Ethics Committee Approval (reference number R14/25) and RCH Human Research Ethics Committee Approval (reference number 24131 G). Blood mononuclear cells were isolated by Ficoll-Paque Plus[TM] density gradient centrifugation (GE Healthcare). Donor thymii were cut into small pieces and passed through a 70 micron cell strainer into ice-cold RPMI-1640 medium containing 2mM EDTA before being washed into PBS + 2% Fetal Calf Serum (FACS buffer).

Magnetic bead enrichment of thymic MAIT cells.

Mouse and human MR1 tetramers were generated and biotinylated as previously described[2,12]. Biotinylated MR1-5-OP-RU or control or Ac-6FP monomers were tetramerized with streptavidin conjugated to either PE (SA-PE) (BD Pharmingen) or Brilliant Violet 421 (SA-BV) (Biolegend). Single cell suspensions of mouse thymus were prepared and stained with PE-mouse MR1-5-OP-RU tetramers prior to magnetic bead enrichment using anti-PE microbeads as per manufacturer's instructions (Miltenyi Biotec). One independent enriched sample contains 5 pooled thymii. Single cell suspensions of human thymus were enriched for Vα7.2$^+$ cells by staining for Vα7.2-PE antibody, followed by magnetic bead enrichment using anti-PE microbeads (Miltenyi Biotec).

Single cell TCR sequencing.

MR1-5-OP-RU tetramer^{+} cells were single cell sorted based on CD24 and CD44 expression and cDNA prepared using SuperScript VILO (Invitrogen) as per manufacturer's instructions. Transcripts encoding different Vα and Vβ genes were amplified using multiplex nested PCR as previously described[27]. PCR products were separated using a 1.5% agarose gel and sequenced by The Molecular Diagnostics Unit, University of Melbourne.

Flow Cytometry.

Mouse and human cells were stained with viability dye 7-aminoactinomycin D (7-AAD; Sigma) and the following cell surface antibodies. Mouse: TCRβ (H57-597, BD Pharmingen), CD4 (RM4-5, Biolegend), CD8 (53-6.7, BD Pharmingen), CD24 (M1/69, BD Pharmingen), CD44 (IM7, BD Pharmingen, eBioscience), CD62L (MEL-14, eBioscience), CD69 (H1.2F3, eBioscience), CD103 (2E7, Biolegend), CD127 (IL-7R A7R34, eBioscience), CD218 (IL-18Rα BG, Biolegend), NK1.1 (PK136, BD Pharmingen) and B220 (RA3-6B2, BD Pharmingen). Human: CD3ε (UCHT1, BD Biosciences), CD4 (OKT4, Biolegend), CD8α (SK1 Biolegend), CD14 (M5E2, Biolegend), CD19 (HIB19, Biolegend), CD27 (O323, Biolegend), CD161 (HP-3G10, Biolegend), IL-18Rα (H44, Biolegend) and Vα7.2 (3C10, Biolegend). Mouse cells are gated on B220^{-} lymphocytes and human cells on CD14^{-} CD19^{-} lymphocytes after dead cell and doublet exclusion. Cells were analysed using a BD LSR Fortessa equipped with a 561nm yellow-green laser and data processed using FlowJo software (Treestar). Mouse MAIT cells were sorted using a BD FACSAriaIII cell sorter.

Intracellular cytokine and intracellular transcription factor staining.

Briefly, magnetic bead enriched MR1-5-OP-RU tetramer^{+} cells from mouse thymus were stimulated for 4h with PMA (10 ng/ml) and ionomycin (1 μg/ml) in the presence of GolgiStop (BD Biosciences). Surface staining of the cells was then performed, before the cells were fixed and permeabilized using BD Cytofix/Cytoperm kit (BD Biosciences) as per manufacturer's instructions. Cells were then stained for intracellular cytokines with anti-IFN-γ (XMG1.2, BD Pharmingen) and anti-IL-17A (TC11-18H10, BD Pharmingen) prior to flow cytometric analysis. PLZF was assessed by staining with the anti-PLZF antibody (Mags.21F7, eBioscience) after the cells were surface-stained and permeabilized with the eBioscience Foxp3 Fixation/Permeabilization kit, according to the manufacturer's instructions.

OP9 co-culture differentiation assay.

To verify the precursor-product relationship of mouse MAIT cells, an adaptation of the OP9 co-culture protocol previously described[25] was used. Briefly, OP9 cells were plated in 96 well plates using DMEM media supplemented with 10% (v/v) Fetal Calf Serum (FCS), 1x GlutaMAX^{TM} (2mM L-Glutamine, Gibco) 15mM HEPES (Gibco), 0.1mM NEAA (non-essential amino acids, Invitrogen), 100U/ml penicillin (sodium salt, Gibco), 1mM sodium pyruvate (Invitrogen), 100µg/ml streptomycin sulfate (Gibco) and 50µM 2-mercaptoethanol (Sigma). 1×10^4 sorted MAIT cells from various stages (Stage 1, 2 and 3) were cultured in the presence or absence of OP9 cells with identical media supplemented with mouse IL-2 (50ng/ml, Peprotech). MR1 blocking antibody (clone 8F2.F9)[28] was added at 10µg/ml. MAIT cells were harvested after 5 days, stained with antibodies and analysed by flow cytometry.

Figure Legends

Figure 1. Identification of distinct MAIT cell subsets in mouse thymus.

Flow cytometry analysis of MR1-5-OP-RU tetramer reactive MAIT cells for expression of CD24, CD44, CD4 and CD8 in adult mouse thymus, spleen, lung and lymph nodes. MR1-Ac-6-FP tetramer was used as a negative control. Data are representative of a total of 6 mice from 3 independent experiments. (b) Phenotypic analysis of $CD24^+CD44^-$ and $CD24^-CD44^+$ thymic MAIT cells with ICOS, CD161 (NK1.1), CD62L, CD69, CD103, CD122 (IL-2R), CD127 (IL-7R) and CD218 (IL-18R), $CD24^+CD44^-$ MAIT cells in blue, $CD24^-CD44^+$ MAIT cells in red, $CD4^+CD8^+$ double positive thymocytes in black. Data from 5 pooled mice from each experiment and is representative of 2 independent experiments for each phenotypic marker. (c) Identification of three populations of thymic MAIT cells following magnetic bead enrichment. Flow cytometry analysis of 3 stages of MAIT cells defined using CD24 and CD44. Stage 1 ($CD24^-CD44^+$) in blue, stage 2 ($CD24^-CD44^-$) in green and stage 3 ($CD24^-CD44^+$) in red. Forward scatter (FSC) and CD4/CD8 co-receptor expression on stage 1, stage 2 and stage 3 MAIT cells. Data are representative of at least 10 independent experiments

Figure 2. Precursor product relationship of mouse MAIT cells

(a) Thymii from 2 week, 4 week and 8-week old C57BL/6 mice were pooled, enriched for $MR1-5-OP-RU$ tetramer$^+$ cells and analyzed for CD24 and CD44 expression. Data are representative of 4 independent samples per age group. (b) Percentages of stage 1, stage 2 and stage 3 MAIT cells in 2 week, 4 week, and 8-week old mice thymii and the bar depicts the mean ± SEM from 4 independent samples. (c) Enriched mouse thymocytes were stimulated for 4h in presence of PMA/ionomycin, labeled with MR1-5-OP-RU tetramer and surface antibodies, fixed and permeabilized and then stained with anti-IFN-γ or IL-17A. Data are representative of 3 independent experiments. (d) $CD24^-CD44^+$ MAIT cells develop from stage 1 $CD24^+CD44^-$ and stage 2 $CD24^-CD44^-$ precursors. Stage 1, stage 2 and stage 3 MAIT cells from Vα19 TCR transgenic (TG) mouse thymii, and stage 1 and stage 3 MAIT cells from wild type mouse thymii, were purified by flow cytometric sorting (day 0) and cultured in the presence or absence of OP9 cells, with or without anti-MR1 antibody. Cultures were harvested on day 5 and MAIT cells examined for CD24 and CD44 expression. Data are representative of 3 independent experiments. (e) Percentages and numbers of stage 3 MAIT cells at the end of culture. Bars depict mean ± SEM for 3 independent experiments.

Figure 3. PLZF controls development of MAIT cells

(a) PLZF expression on stage 1, stage 2 and stage 3 cells from enriched C57BL/6 wild type (WT) mouse thymus. (b) Analysis of MAIT cells from spleen, lymph node or enriched thymus from C57BL/6 WT and PLZF knockout (KO) mice. Cells were examined for CD24, CD44, and CD4/CD8 co-receptor expression using flow cytometry. Data are representative of 3 independent experiments with a total of 9 mice per group. (c) Percentages of stage 1, stage 2 and stage 3 MAIT cells in enriched thymus, spleen and lymph nodes of WT and PLZF KO mice. Bars depict mean ± SEM, data are representative of 3 independent experiments with a combined total of 9 mice per group *P<0.1 **P<0.01 ***P<0.001 using a Mann-Whitney rank sum U test.

Figure 4. Identification of distinct MAIT cell subsets in humans

(a) Flow cytometric analysis of adult peripheral blood samples, human thymus samples enriched for Vα7.2$^+$ cells, young peripheral blood samples matched from the thymus donors, and donor cord bloods. The first two panels depict CD3$^+$ lymphocytes, stained with anti-Vα7.2 and either MR1-Ac-6FP or MR1-5-OP-RU tetramer. In the next three panels, CD3$^+$ Vα7.2$^+$ MR1-5-OP-RU tetramer$^+$ MAIT cells were analyzed for CD4, CD8, CD161, CD218 and CD27 expression. (b) Graph depicts percentage MR1-5-OP-RU tetramer$^+$ cells of total Vα7.2$^+$ population in thymus, cord blood, young and adult peripheral blood. Data shows 9 samples for cord, young and adult blood and 12 thymus samples. (c) Percentages of CD161$^-$CD218$^-$ subset of total MAIT cells in thymus, cord blood, young and adult peripheral blood. Sample size as per b. (d) Percentages of CD4$^+$CD8$^+$, CD4$^+$CD8$^-$, and CD4$^-$CD8$^+$ MAIT cells in human thymus and young peripheral blood. Donor matched samples are indicated with a line. Data shows 9 samples for young peripheral blood and 12 thymus samples *<0.1 **P<0.01 ***P<0.001 using a Mann-Whitney rank sum U test. (e) Percentages of CD27$^-$CD161$^-$, CD27$^+$CD161$^-$, and CD161$^+$ MAIT cells from 5 thymus samples, 4 cord blood samples and peripheral blood samples from 4 young and 5 adult donors. (f) CD4/CD8 co-receptor and PLZF expression on stage 1 (CD161$^-$CD27$^-$) cells in blue, stage 2 (CD161$^-$CD27$^+$) cells in green and stage 3 cells (CD161$^+$CD27$^{-/+}$) in red.

References

1   Treiner, E. *et al.* Selection of evolutionarily conserved mucosal-associated invariant T cells by MR1. *Nature* **422**, 164-169 (2003).

2   Corbett, A. J. *et al.* T-cell activation by transitory neo-antigens derived from distinct microbial pathways. *Nature* **509**, 361-365, doi:10.1038/nature13160 (2014).

3   Kjer-Nielsen, L. *et al.* MR1 presents microbial vitamin B metabolites to MAIT cells. *Nature* **491**, 717-723, doi:10.1038/nature11605 (2012).

4   Tilloy, F. *et al.* An invariant T cell receptor alpha chain defines a novel TAP-independent major histocompatibility complex class Ib-restricted alpha/beta T cell subpopulation in mammals. *J Exp Med* **189**, 1907-1921 (1999).

5   Dusseaux, M. *et al.* Human MAIT cells are xenobiotic-resistant, tissue-targeted, CD161hi IL-17-secreting T cells. *Blood* **117**, 1250-1259, doi:10.1182/blood-2010-08-303339 (2011).

6   Le Bourhis, L. *et al.* Antimicrobial activity of mucosal-associated invariant T cells. *Nat Immunol* **11**, 701-708, doi:ni.1890 [pii] 10.1038/ni.1890 (2010).

7   Tang, X. Z. *et al.* IL-7 Licenses Activation of Human Liver Intrasinusoidal Mucosal-Associated Invariant T Cells. *J Immunol* **190**, 3142-3152, doi:10.4049/jimmunol.1203218 (2013).

8   Martin, E. *et al.* Stepwise Development of MAIT Cells in Mouse and Human. *PLoS Biol* **7**, e54 (2009).

9   Gold, M. C. *et al.* Human mucosal associated invariant T cells detect bacterially infected cells. *PLoS Biol* **8**, e1000407, doi:10.1371/journal.pbio.1000407 (2010).

10   Meierovics, A., Yankelevich, W. J. & Cowley, S. C. MAIT cells are critical for optimal mucosal immune responses during in vivo pulmonary bacterial infection. *Proc Natl Acad Sci U S A* **110**, E3119-3128, doi:10.1073/pnas.1302799110 (2013).

11   Seach, N. *et al.* Double-positive thymocytes select mucosal-associated invariant T cells. *J Immunol* **191**, 6002-6009, doi:10.4049/jimmunol.1301212 (2013).

12   Eckle, S. B. *et al.* A molecular basis underpinning the T cell receptor heterogeneity of mucosal-associated invariant T cells. *J Exp Med* **211**, 1585-1600, doi:10.1084/jem.20140484 (2014).

13   Reantragoon, R. *et al.* Antigen-loaded MR1 tetramers define T cell receptor heterogeneity in mucosal-associated invariant T cells. *J Exp Med* **210**, 2305-2320, doi:10.1084/jem.20130958 (2013).

14   Benlagha, K., Wei, D. G., Veiga, J., Teyton, L. & Bendelac, A. Characterization of the early stages of thymic NKT cell development. *J Exp Med* **202**, 485-492 (2005).

15   Rahimpour, A. *et al.* Identification of phenotypically and functionally heterogeneous mouse Mucosal Associated Invariant T cells using MR1-antigen tetramers. *J. Exp. Med.* **in press** (2015).

16   Schmitt, T. M. & Zuniga-Pflucker, J. C. Induction of T cell development from hematopoietic progenitor cells by delta-like-1 in vitro. *Immunity* **17**, 749-756 (2002).

17   Ciofani, M., Knowles, G. C., Wiest, D. L., von Boehmer, H. & Zuniga-Pflucker, J. C. Stage-specific and differential notch dependency at the alphabeta and gammadelta T lineage bifurcation. *Immunity* **25**, 105-116, doi:10.1016/j.immuni.2006.05.010 (2006).

18   Constantinides, M. G., McDonald, B. D., Verhoef, P. A. & Bendelac, A. A committed precursor to innate lymphoid cells. *Nature* **508**, 397-401, doi:10.1038/nature13047 (2014).

19   Kovalovsky, D. *et al.* The BTB-zinc finger transcriptional regulator PLZF controls the development of invariant natural killer T cell effector functions. *Nat Immunol* **9**, 1055-1064, doi:ni.1641 [pii] 10.1038/ni.1641 (2008).

20   Kreslavsky, T. *et al.* TCR-inducible PLZF transcription factor required for innate phenotype of a subset of {gamma}{delta} T cells with restricted TCR diversity. *Proc Natl Acad Sci U S A* **106**, 12453-12458 (2009).

21   Savage, A. K. *et al.* The Transcription Factor PLZF Directs the Effector Program of the NKT Cell Lineage. *Immunity* **29**, 391-403 (2008).

22   Fergusson, J. R. *et al.* CD161 defines a transcriptional and functional phenotype across distinct human T cell lineages. *Cell reports* **9**, 1075-1088, doi:10.1016/j.celrep.2014.09.045 (2014).

23   Walker, L. J. *et al.* Human MAIT and CD8alphaalpha cells develop from a pool of type-17 precommitted CD8+ T cells. *Blood* **119**, 422-433, doi:10.1182/blood-2011-05-353789 (2012).

24   Lepore, M. *et al.* Parallel T-cell cloning and deep sequencing of human MAIT cells reveal stable oligoclonal TCRbeta repertoire. *Nature communications* **5**, 3866, doi:10.1038/ncomms4866 (2014).

25   Berzins, S. P., Cochrane, A. D., Pellicci, D. G., Smyth, M. J. & Godfrey, D. I. Limited correlation between human thymus and blood NKT cell content revealed by an ontogeny study of paired tissue samples. *Eur J Immunol* **35**, 1399-1407 (2005).

26   Leeansyah, E., Loh, L., Nixon, D. F. & Sandberg, J. K. Acquisition of innate-like microbial reactivity in mucosal tissues during human fetal MAIT-cell development. *Nature communications* **5**, 3143, doi:10.1038/ncomms4143 (2014).

27   Wang, G. C., Dash, P., McCullers, J. A., Doherty, P. C. & Thomas, P. G. T cell receptor alphabeta diversity inversely correlates with pathogen-specific antibody levels in human cytomegalovirus infection. *Science translational medicine* **4**, 128ra142, doi:10.1126/scitranslmed.3003647 (2012).

28   Chua, W. J. *et al.* Endogenous MHC-related protein 1 is transiently expressed on the plasma membrane in a conformation that activates mucosal-associated invariant T cells. *Journal of immunology* **186**, 4744-4750, doi:10.4049/jimmunol.1003254 (2011).
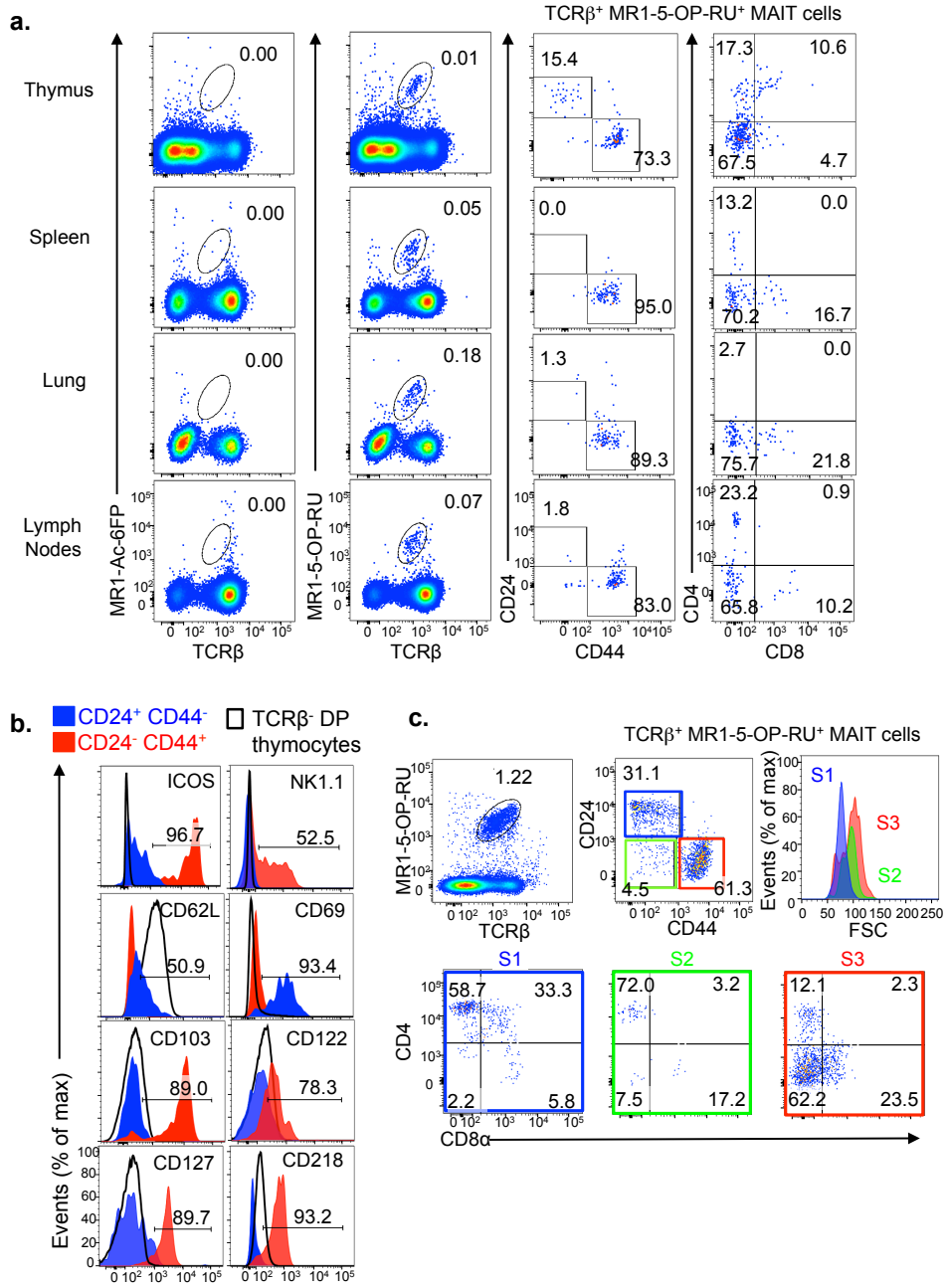
FIGURE 1

a.

TCRβ⁺ MR1-5-OP-RU⁺ MAIT cells

Thymus | Spleen | Lung | Lymph Nodes

(MR1-Ac-6FP vs TCRβ, MR1-5-OP-RU vs TCRβ, CD24 vs CD44, CD4 vs CD8)

b.
- CD24⁺ CD44⁻ (blue)
- CD24⁻ CD44⁺ (red)
- TCRβ⁻ DP thymocytes (open)

Markers: ICOS (96.7), NK1.1 (52.5), CD62L (50.9), CD69 (93.4), CD103 (89.0), CD122 (78.3), CD127 (89.7), CD218 (93.2)

Events (% of max)

c.

TCRβ⁺ MR1-5-OP-RU⁺ MAIT cells

S1, S2, S3 populations

CD4 vs CD8α
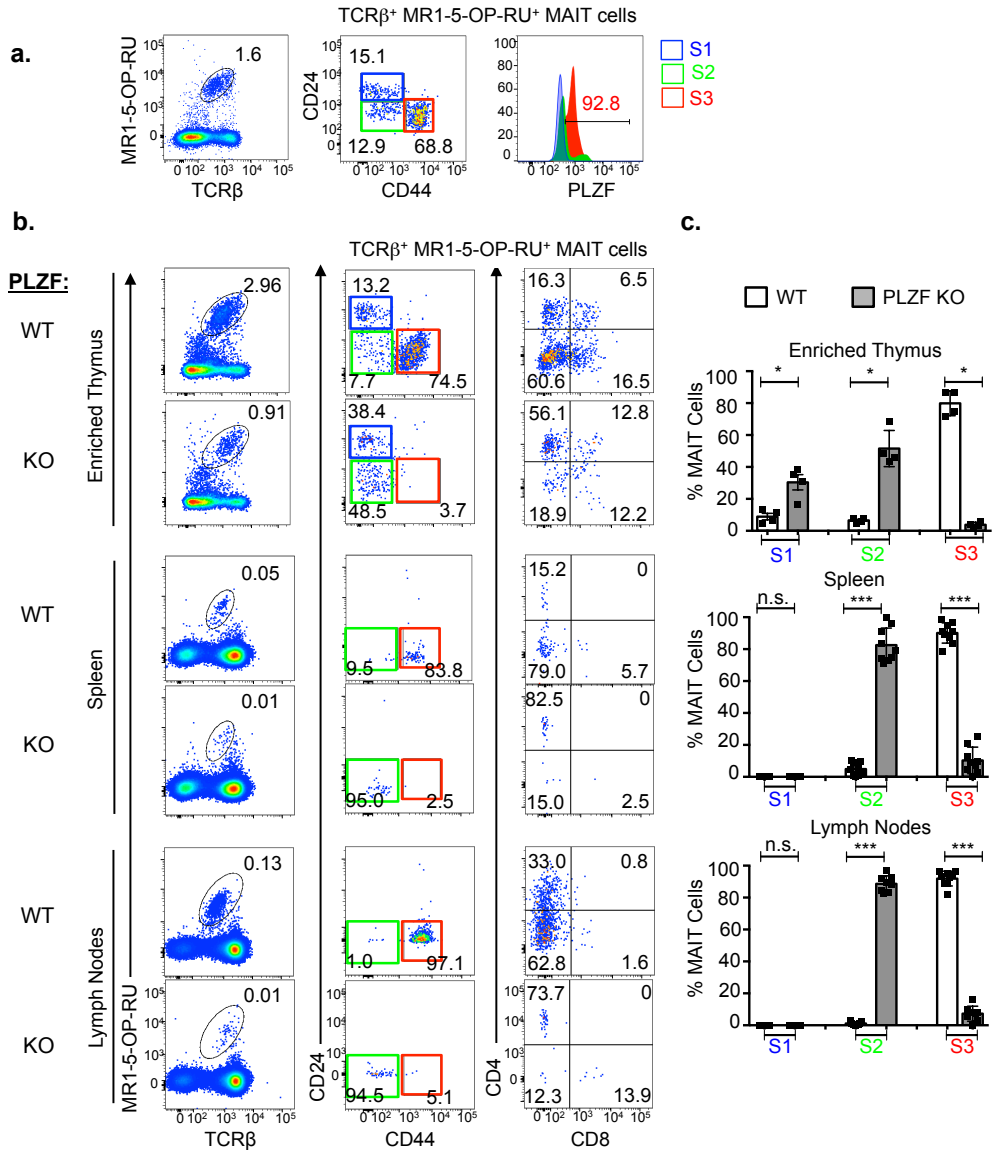
FIGURE 2

FIGURE 3

FIGURE 4
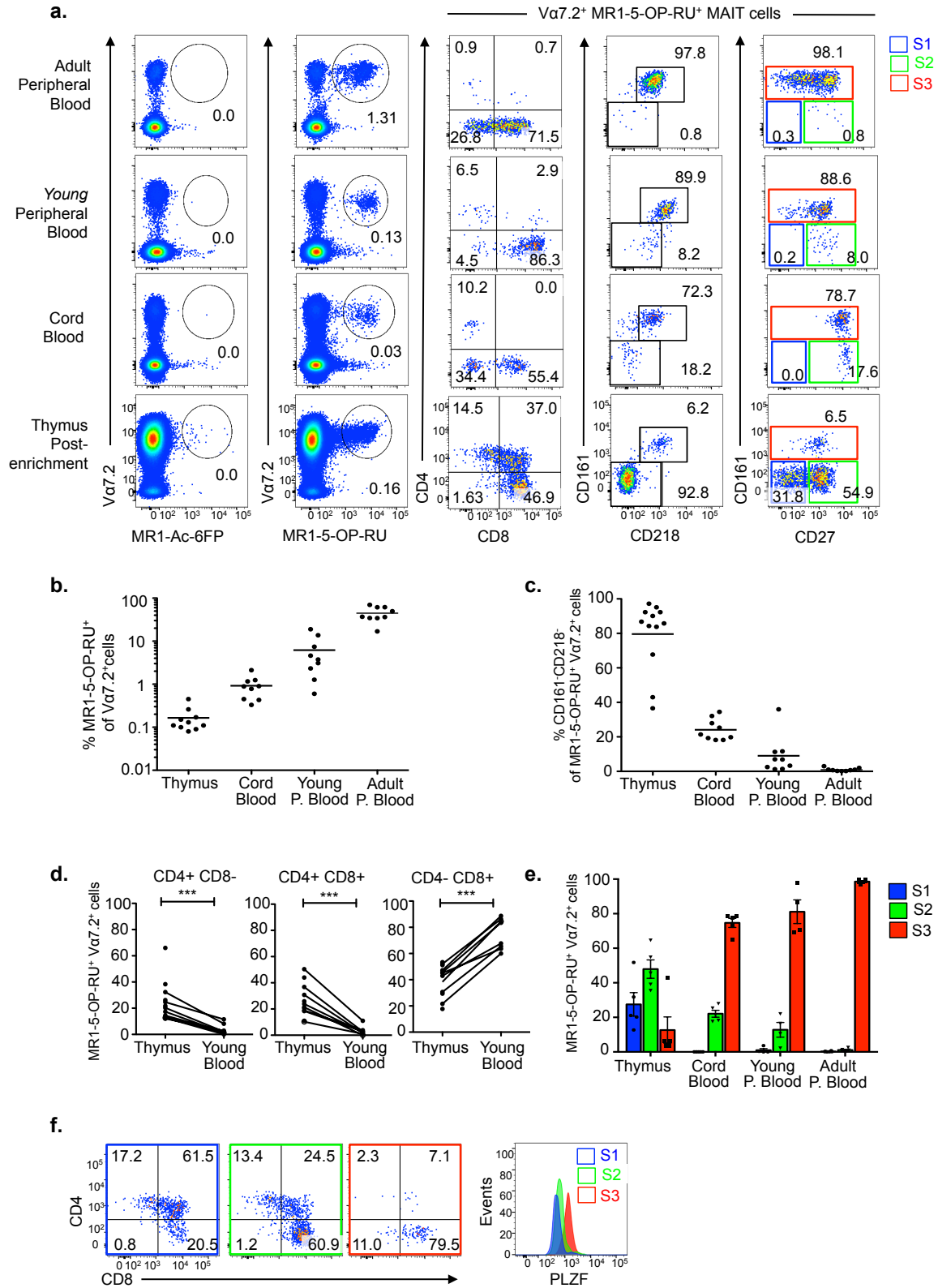
Supplementary Table 1

Cell	TRAV	TRAJ	CDR3 alpha	TRBV	TRBJ	CDR3 beta
			Stage 1 CD24+ CD44- MR1-5-OP-RU+ TCRβ+			
1	TRAV1	TRAJ33	CAVRDSNYQLIW	TRBV13	TRBJ1-3	CASGDASXSGNTLYF
2	TRAV1	TRAJ33	CAVTDSNYQLIW	TRBV13-3	TRBJ2-1	CASSEQGGYAEQFF
3	TRAV1	TRAJ33	CAVRDSNYQLIW	TRBV13-2	TRBJ2-5	CASGGWGFQDTQYF
4	TRAV1	TRAJ33	CAVRXXNYXLIW	TRBV13-3		N.D.
5	TRAV1	TRAJ33	CAVRDRDYQLIW	TRBV19	TRBJ1-6	
6	i) TRAV1 ii) TRAV9	i) TRAJ33 ii) TRAJ29	CAPMDSNYQLXW	TRBV13-2		N.D.
7	i) TRAV1 ii) TRAV7	TRAJ33	CAVRDSNYQLIW	TRBV13-2	TRBJ2-5	CASGDGGGWDTQYF
8	TRAV1	TRAJ33	CAVRDSNYQLIW	TRBV13-3	TRBJ1-6	CASSDAGVNSPLYF
9	TRAV1	TRAJ33	CAVSNSNYQLIW	TRBV13-2	TRBJ2-1	CASGDGDSYAEQFF
10	TRAV1	TRAJ33	CAVRDSNYQLIW	TRBV13-2	TRBJ2-3	CASGDGDSAETLYF
11	TRAV1	TRAJ33	CAVRDSNYQLIW	TRBV13-2	TRBJ2-3	CASGGDGDSAETLYF
12	TRAV1	TRAJ33	CAVMDSNYQLIW	TRBV13-2	TRBJ2-1	CASGDGDSYAEQFF
13	TRAV1	TRAJ33	CAVRDSNYQLIW	TRBV13-3	TRBJ2-7	CASSAGTSSYEQYF
			Stage 3 CD24- CD44+ MR1-5-OP-RU+ TCRβ+			
14	TRAV1	TRAJ33	CAVRDSNYQLIW	TRBV13-3	TRBJ2-2	CASSDKGDTGQLYF
15	TRAV1	TRAJ33	CAVLDSNYQLIW	TRBV13-3	TRBJ1-6	CASSDAGVNSPLYF
16	TRAV1	TRAJ33	CAVMDSNYQLIW	TRBV19	TRBJ2-7	CASSPGLESSYEQYF
17	TRAV1	TRAJ33	CAVKDSNYXLIW	TRBV13-3	TRBJ2-2	CASTRTENTGQLYF

TCR sequences of mouse MAIT cell subsets.

MR1-5-OP-RU tetramer^{+} stage 1 CD24^{+}CD44^{-} and stage 3 CD24^{-}CD44^{+} MAIT cells were sorted as single cells and their TCR-α and β chains were determined using single cell TCR sequencing. X defines undetermined amino acid.

Supplementary Table 2

	Stage 1 CD24$^+$CD44$^-$	Stage 3 CD24$^-$CD44$^+$
CD4 and CD8	CD4 or CD4$^+$CD8$^+$	CD4$^+$ or CD8$^+$ or CD4$^-$CD8$^-$
PLZF	Negative/low	Positive
CD161 (NK1.1)	Negative/low	Low to Positive
CD62L	Intermediate	Negative
CD69	Positive	Negative
CD103	Negative	Mostly Positive
CD122 (IL-2R)	Negative	Intermediate
CD127 (IL-7R)	Negative	Positive
CD218 (IL-18R)	Negative	Positive
CD278 (ICOS)	Negative/low	Positive

Phenotypic characteristics of stage 1 and stage 3 MAIT cells in mice.
Stage 1 and stage 3 MAIT cells were labeled with antibodies for a panel of phenotypic markers and analyzed by flow cytometry.
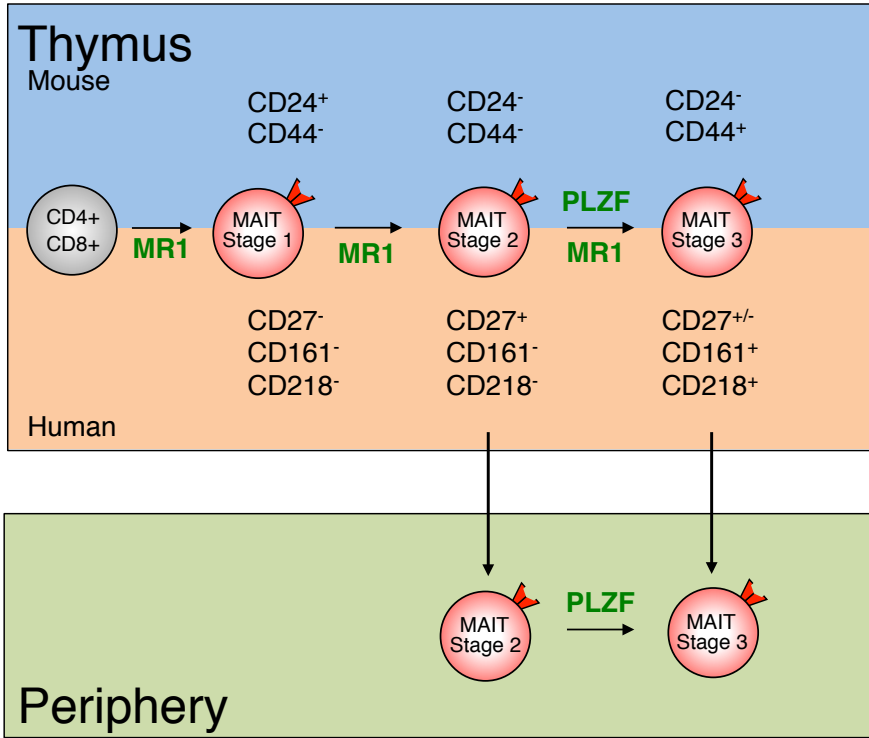
Supplementary Figure 1
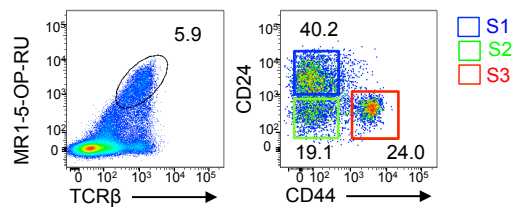
Thymic MAIT cell subsets in Vα19 transgenic mice.
Flow cytometry analysis of MR1-5-OP-RU tetramer reactive MAIT cells for expression of CD24 and CD44 in adult Vα19 transgenic mouse thymus. Data are representative of 3 independent experiments.

Supplementary Figure 2

Schematic of the MAIT cell development pathway.